Development 139, 1821-1830 (2012) doi:10.1242/dev.075796

Wnt9b-dependent FGF signaling is crucial for outgrowth of the nasal and maxillary processes during upper jaw and lip development

Yong-Ri Jin[1], Xiang Hua Han[1], Makoto M. Taketo[2] and Jeong Kyo Yoon[1,*]

SUMMARY

Outgrowth and fusion of the lateral and medial nasal processes and of the maxillary process of the first branchial arch are integral to lip and primary palate development. *Wnt9b* mutations are associated with cleft lip and cleft palate in mice; however, the cause of these defects remains unknown. Here, we report that *Wnt9b*$^{-/-}$ mice show significantly retarded outgrowth of the nasal and maxillary processes due to reduced proliferation of mesenchymal cells, which subsequently results in a failure of physical contact between the facial processes that leads to cleft lip and cleft palate. These cellular defects in *Wnt9b*$^{-/-}$ mice are mainly caused by reduced FGF family gene expression and FGF signaling activity resulting from compromised canonical WNT/β-catenin signaling. Our study has identified a previously unknown regulatory link between WNT9B and FGF signaling during lip and upper jaw development.

KEY WORDS: WNT, β-Catenin, FGF signaling, Orofacial morphogenesis, Cleft lip, Cleft palate, Mouse

INTRODUCTION

Upper lip and nose development in mice starts around embryonic day (E) 9.5, when neural crest cells from the dorsal region of the fore- and mid-brain migrate ventrally and form mesenchyme within an unpaired frontonasal prominence rostral to the telencephalon (Serbedzija et al., 1992; Osumi-Yamashita et al., 1994; Kontges and Lumsden, 1996; Creuzet et al., 2005; Minoux and Rijli, 2010). In parallel, maxillary processes (MxPs) derived from the first branchial arch (BA1) become evident lateral to the stomodeum and rostral to the mandibular processes (MdPs). At E10, within the ventrolateral region of the frontonasal prominence, the medial nasal (MNP) and lateral nasal (LNP) processes bulge and outgrow around the periphery of the nasal placode in a horseshoe shape, forming the nasal pit. In the E10.5 mouse embryo, mesenchymal cells within the MNP, LNP and MxP divide rapidly (Jiang et al., 2006). The lateral growth of the MxP pushes the nasal pits toward the middle face region. The ventral tip of the MNP extends further rostrally and ventrolaterally to begin fusion with both the LNP and the MxP at the medial end of their boundary junction. During fusion of these processes, apoptosis of epithelial cells occurs in the seam of the contacting MNP and LNP, resulting in the connection of mesenchymal cell compartments. By E11.5, the nostrils and lip are correctly formed by the completion of fusion of the MNP, LNP and MxP (Jiang et al., 2006; Song et al., 2009). In addition, the expanding MxP pushes the nostrils into the more medial region. Failure or delay of outgrowth and fusion of the NPs and MxP lead to cleft lip with or without cleft palate (CL/P) (Szabo-Rogers et al., 2010; Dixon et al., 2011).

The significance of the WNT signaling pathway in regulating facial morphogenesis is suggested by expression of various WNT ligand genes within the facial prominences (Summerhurst et al., 2008; Geetha-Loganathan et al., 2009). Canonical WNT signaling reporter transgenes such as *TopGAL*, *BATgal* and *Axin2-lacZ* are highly expressed in the facial prominences and their derivatives, further indicating a potential role of WNT/β-catenin signaling during facial development (Maretto et al., 2003; Brugmann et al., 2007; Al Alam et al., 2011).

Previous studies of genetically altered mice in which the key components of WNT signaling are disrupted further suggest the crucial roles of WNT signaling in facial development. For instance, ablation of the canonical WNT signaling receptor gene *Lrp6* causes hypoplasia of the facial processes accompanied by reduced cell proliferation within the NPs and CL/P in mice (Song et al., 2009). These mutant mice display severely reduced WNT/β-catenin signaling activity and decreased expression of the WNT target genes *Msx1* and *Msx2* within the facial processes.

Both inactivation and constitutive activation of *Ctnnb1*, which encodes β-catenin, a central mediator of canonical WNT signaling, in the embryonic facial domains result in severe facial defects (Brault et al., 2001; Reid et al., 2011; Wang et al., 2011). Facial ectoderm-specific deletion or activation of *Ctnnb1* result in downregulation or upregulation, respectively, of ectodermal FGF family gene expression, showing that canonical WNT signaling controls ectoderm FGF signaling during facial development (Reid et al., 2011; Wang et al., 2011). Mice lacking the R-spondin 2 (*Rspo2*) gene, which encodes a novel WNT agonist, exhibit hypoplasia and disrupted patterning of the MdP, and cleft of the secondary palate with very low penetrance of cleft lip (Yamada et al., 2009; Jin et al., 2011).

Among the WNT genes expressed in the facial prominences, the developmental function of the individual genes and their association with craniofacial abnormalities including CL/P are not fully understood (Menezes et al., 2010). *Wnt3* and *Wnt9b* are suggested to play roles in CL/P. Homozygous *WNT3* mutation in humans is associated with CL/P (Niemann et al., 2004). The

[1]COBRE in Stem Cell and Regenerative Medicine, Center for Molecular Medicine, Maine Medical Center Research Institute, Maine Medical Center, 81 Research Drive, Scarborough, ME 04074, USA. [2]Department of Pharmacology, Graduate School of Medicine, Kyoto University, Yoshida-Konoé-Cho, Sakyo-Ku, Kyoto, Japan.

*Author for correspondence (yoonje@mmc.org)

Accepted 29 February 2012

association of *Wnt9b* with CL/P arises from the study of A/WySn mice. Approximately 5-30% of A/WySn mice display CL/P and the two genetic loci, *clf1* and *clf2*, have been identified by linkage to CL/P. The *clf1* locus is located in the proximity of *Wnt9b* (Juriloff et al., 2005). By genetic complementation, A/WySn mice were confirmed to be homozygous for a hypomorphic *Wnt9b* allele (Juriloff et al., 2006). Consistent with the A/WySn study, *Wnt9b* null mice also show a higher frequency of CL/P than A/WySn mice (Juriloff et al., 2006). However, the nature of the embryological defects in *Wnt9b* null mice that lead to CL/P and the mechanism by which *Wnt9b* regulates the morphogenesis of facial structures during embryogenesis remain unknown.

In the present study, we investigated facial morphogenesis in *Wnt9b* null embryos. We found that loss of the *Wnt9b* gene caused retarded outgrowth and failed contact of the NPs and MxP, resulting in CL/P at a later stage. These defects were a direct consequence of reduced cell proliferation without any notable increase of cell apoptosis within mesenchymal cells of the NPs and MxP. Furthermore, these defects were associated with downregulation of FGF signaling, which acts as a mitogenic signal for mesenchymal cells in the NPs and MxP, as a result of compromised WNT/β-catenin signaling in $Wnt9b^{-/-}$ embryos. Our findings have identified a previously unknown role of *Wnt9b* in regulating the proliferation of NP and MxP mesenchymal cells by positively modulating ectoderm-derived FGF signaling.

MATERIALS AND METHODS

Animals

Mice carrying the *Wnt9b* conditional null ($Wnt9b^{loxp/loxp}$) allele (Carroll et al., 2005) in a genetic background outcrossed with Swiss Webster were kindly provided by Thomas J. Carroll (University of Texas Southwestern Medical Center). We crossed these mice with C57BL/6 mice once and the offspring were maintained in the mixed genetic background. A null allele of *Wnt9b* was generated by crossing $Wnt9b^{+/loxp}$ mice with *CMV-Cre* transgenic mice (Nagy et al., 1998). *TopGAL* (DasGupta and Fuchs, 1999) and $Foxg1^{+/Cre}$ mice (Hebert and McConnell, 2000) were obtained from The Jackson Laboratory. $Ctnnb1^{+/loxp(Ex3)}$ mice carrying a conditional allele of constitutively active β-catenin (Harada et al., 1999) was obtained from Terry Yamaguchi (National Cancer Institute-Frederick). Mice were genotyped by PCR as described (Hebert and McConnell, 2000; Dunty et al., 2008; Jin et al., 2011). For in vivo activation of WNT/β-catenin signaling, 60 μl 300 mM LiCl or control 300 mM NaCl solution were intraperitoneally injected into pregnant females consecutively at gestation days 8.5, 9.5 and 10 before harvesting embryos at E10.5. Mice were housed in a pathogen-free air barrier facility. Animal handling and procedures were approved by the Maine Medical Center Institutional Animal Care and Use Committee.

Skeletal preparation, β-galactosidase staining and whole-mount in situ hybridization

Skeletal preparation and measurement, whole-mount β-galactosidase staining using X-Gal substrate, and whole-mount in situ hybridization were performed as described (Jin et al., 2011). The stained embryos were processed for cryosections. Fetuses/embryos and the cryosections were photographed using a Zeiss StemiSV6 stereomicroscope and Zeiss Axioskop microscope with a Zeiss AxioCam digital camera.

Scanning electron microscopy

Embryos were fixed with 2% glutaraldehyde/2% paraformaldehyde in PBS buffer followed by OsO_4 and gradually dehydrated in ethanol. The embryos were critical point dried under CO_2 and sputter coated with 30 nm gold particles. Images were obtained using an AMRay 1000 scanning electron microscope (Gold International Machinery) and iXRF digital capture system at the Scanning Electron Microscopy Facility of the University of Maine at Orono.

BrdU incorporation and apoptosis assays and immunofluorescence staining

For BrdU incorporation assays, pregnant mice (E10.5 or E13.5) were intraperitoneally injected with BrdU (100 mg/kg body weight, Invitrogen) for 15 (E10.5-11 embryos) or 30 (E13.5 embryos) minutes prior to sacrifice. The incorporated BrdU was detected immunohistochemically in cryosections using a cell proliferation kit (Invitrogen). Apoptotic cells were detected in TdT-mediated dUTP nick-end labeling (TUNEL) assay using an in situ cell death detection kit (Roche Applied Science). Immunofluorescence staining with anti-phospho-histone H3 (1:100 dilution, Cell Signaling), anti-activated caspase 3 (1:100, Cell Signaling) and anti-PY489-β-catenin (1:100, Developmental Studies Hybridoma Bank) was performed on cryosections.

qRT-PCR and western blot analysis

Total RNA was isolated at least in triplicate from NP/MxP tissues freshly dissected from embryos and from cultured NP/MxP explants using Trizol (Sigma). Quantitative real-time (qRT) PCR using cDNA (10 ng total RNA equivalent) synthesized using the Proscript cDNA Synthesis Kit (New England Biolabs) was performed in duplicate per sample as described (Jin et al., 2011). Expression level was normalized to *Gapdh* and E-cadherin (*Cdh1*; when epithelium-specific genes were examined). PCR primers are listed in supplementary material Table S1 and as described previously (Jin et al., 2011).

Protein lysates (10 μg), prepared by homogenizing the tissues or cultured cells in RIPA lysis buffer [10 mM Tris-Cl pH 7.2, 2 mM EDTA, 150 mM NaCl, 1% Nonidet P40, 0.1% SDS, 50 mM NaF, 1% sodium deoxycholate, 1 mM PMSF, 1× protease inhibitor mixture set V (EMD Chemicals), 0.2 mM sodium vanadate] were used in western blot analysis. Primary antibodies (all 1:1000 dilution) were against phospho-LRP6 (Cell Signaling), LRP6 (Santa Cruz Biotechnology), phospho-c-JUN (Cell Signaling), phospho-JNK1/2 (Cell Signaling), JNK1/2 (Cell Signaling), phospho-ROCK2 (Abcam), ROCK2 (Santa Cruz Biotechnology), phospho-ERK1/2 (Cell Signaling), ERK1/2 (Cell Signaling) and α-tubulin (Santa Cruz Biotechnology). The horseradish peroxidase (HRP) signal conjugated with secondary antibodies was developed using the Super Signal West Dura Kit (Thermo Scientific/Pierce). The signals were quantified using ImageJ software, and each experiment was performed in triplicate.

RHOA family small GTPase assays

The small GTPase assay was performed using the RHOA and RAC1/CDC42 activation assay kit (Millipore) according to the manufacturer's instructions. Briefly, NP/MxP tissues were dissected in cold PBS from E10.5 wild-type or mutant embryos (n=7) and homogenized in lysis buffer comprising 20 mM HEPES (pH 7.4), 50 mM NaF, 0.2 mM $MgCl_2$, 20% glycerol, 0.1% Triton X-100, 1 mM PMSF, 0.2 mM sodium orthovanadate and 1× protease inhibitor cocktail set V (EMD Chemicals). Lysates (500 μg) prepared in duplicate (14 wild-type and 14 mutant embryos, total) were used for detection of the activated RHOA family small GTPase. Positive controls were produced by adding GTP into the lysates to activate the GTPases.

Palate shelf and facial process explant and primary mesenchymal cell culture

Palatal organ culture was performed as described (Jin et al., 2011). For facial process explant culture, NP/MxP tissues were dissected in cold PBS from E10.5 or E11-11.5 (for ex vivo NP/MxP fusion assay) embryos and cultured for up to 36 hours on filters floating in Transwell plates (Corning) filled with α-MEM medium with 0.1 μg/ml ascorbic acid, 10% fetal bovine serum (FBS) and streptomycin/penicillin. When indicated, the ectodermal layer was removed by incubating the explants with dispase II (2.4 units/ml, Roche Applied Science) for 30 minutes.

Mesenchymal cells of the facial processes were prepared and cultured as previously described (Song et al., 2009) with minor modifications. After the ectodermal layer was removed by dispase II treatment, the NP/MxP mesenchymal tissues were digested in 0.25% trypsin solution on ice overnight. A single-cell suspension was obtained by gentle pipetting several times, and the cells were cultured in DMEM with 20% FBS. Recombinant

FGFs and WNT9B proteins (R&D) were added to the culture medium as indicated. NP603 (EMD Chemicals), a specific FGF receptor inhibitor, was resuspended in DMSO and added to culture medium at 5 μM.

Cell proliferation and migration assays

For the cell proliferation assay, 1×10^5 cells were seeded in each well of 6-well plates (Nunc) in triplicate. After 3 days in culture, total cell number was determined using a Vi-Cell automated cell viability analyzer (Beckman Coulter). For the wound-healing assay, 1×10^6 cells were seeded and cultured in 6-well plates overnight. The surface of the cell layer was scratched with a 1-ml pipette tip, followed by washing with PBS, and fresh medium containing FGF or WNT9B proteins was added. Phase-contrast images were taken after culturing cells for 16 hours. For the migration assay, 4×10^4 cells were seeded on top of the filter (8 μm pore size) of 96-well Transwell plates (Corning). DMEM containing control bovine serum albumin (400 ng/ml) or WNT9B (400 ng/ml) protein was added into the bottom chambers (n=6). After 8 hours of culture, migrated cells were counted after DAPI staining.

Sample numbers and statistical analysis

Three or four embryos or fetuses of each genotype were used in experiments unless indicated otherwise. The experimental data were analyzed using a non-paired Student's t-test. Statistical significance was set at $P<0.05$.

RESULTS

Wnt9b null mice display CL/P and skeletal abnormalities in the upper jaw

To determine the function of *Wnt9b* during facial development, we examined the craniofacial morphology of *Wnt9b*$^{-/-}$ mice at E18.5. Consistent with previous reports, *Wnt9b*$^{-/-}$ mice developed CL/P (unilateral CL/P, n=2/15; bilateral CL/P, n=13/15) (Fig. 1A-D), confirming that *Wnt9b* is required for proper development of the lip and palate. The penetrance of the CL/P phenotype in *Wnt9b*$^{-/-}$ mice was 100% in the mixed genetic background, which is higher than previously reported (Carroll et al., 2005; Juriloff et al., 2006), probably owing to different genetic backgrounds.

Histological analyses during palatogenesis showed that initial downward growth of the palatal shelves occurred normally in *Wnt9b*$^{-/-}$ mice at E12.5-13.5 (supplementary material Fig. S1E,F). A failure or delay of horizontal elevation of the palatal shelves that subsequently led to failed midline contact was observed in *Wnt9b*$^{-/-}$ mice at E14.5 (Fig. 1E,F). No apparent defects in cell proliferation (supplementary material Fig. S1A-C) or apoptosis (data not shown) within the palatal shelves or in their fusion ability (supplementary material Fig. S1G-J) were observed in *Wnt9b*$^{-/-}$ mice, indicating that palatogenesis defects in *Wnt9b*$^{-/-}$ mice are not intrinsic to the palatal shelves. These results are consistent with the absence of *Wnt9b* expression in the palate shelves (Lan et al., 2006; He et al., 2011).

We analyzed craniofacial bone and cartilage structures in *Wnt9b*$^{-/-}$ mice at E18.5. There was no obvious difference in the dimension of the skull, including length and width, in *Wnt9b*$^{-/-}$ mice (Fig. 1G,H; supplementary material Fig. S2). However, several skeletal components of the upper jaw were either missing or malformed (Fig. 1I-L). For instance, the premaxilla (pmx) of *Wnt9b*$^{-/-}$ mice was much smaller than that of wild-type mice and failed to connect. The palatine processes of both premaxilla and maxilla (pppx and ppmx) were underdeveloped and remained unfused (n=12/12). Interestingly, although some *Wnt9b*$^{-/-}$ mice displayed unilateral cleft lip, their primary palate skeleton, including pppx and ppmx, was defective bilaterally. Taken together, loss of *Wnt9b* caused CL/P with developmental defects of the upper jaw skeleton.

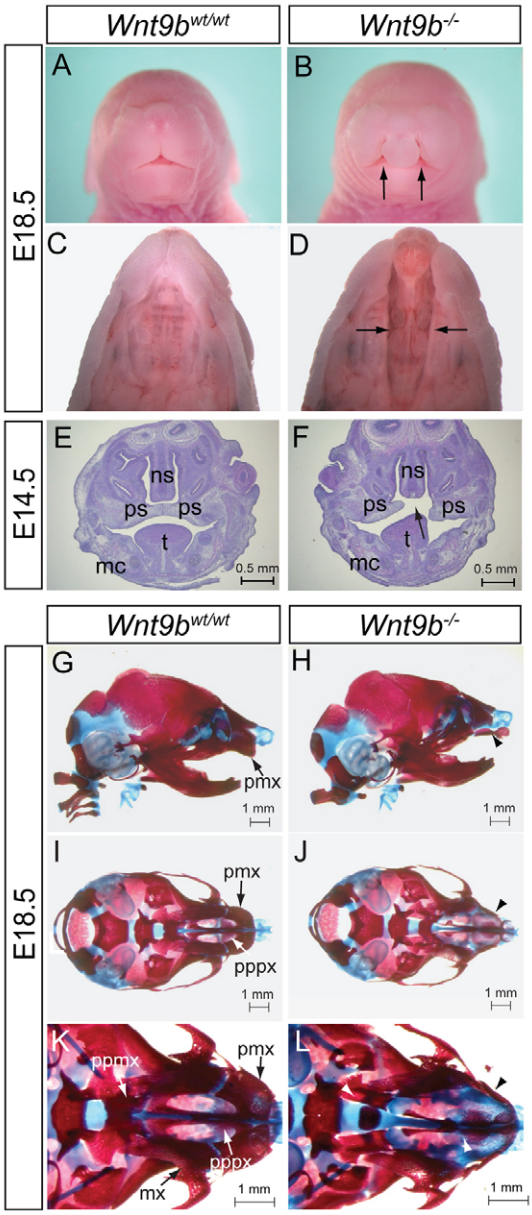

Fig. 1. Cleft lip with cleft palate (CL/P) and craniofacial skeletal defects in *Wnt9b*$^{-/-}$ mice. (**A**,**B**) Front facial views of wild-type and *Wnt9b*$^{-/-}$ fetuses at E18.5. Arrows indicate the bilateral cleft lip. (**C**,**D**) Ventral view of the lip and palate in E18.5 fetuses. The lower jaw was removed for a better view of the palate. Cleft of the secondary palate is indicated by arrows. (**E**,**F**) Coronal sections of the facial region of E14.5 embryos. Arrow indicates cleft of the secondary palate. (**G-L**) Lateral (G,H) and ventral (I-L) views of wild-type and *Wnt9b*$^{-/-}$ skulls at E18.5. The mandible was removed for a better view of the skull in I-L. The pmx bone is well developed in wild-type mice, whereas *Wnt9b*$^{-/-}$ pmx bone is underdeveloped and separated into two pieces due to cleft lip (arrowheads). mc, Meckel's cartilage; mx, maxillar; ns, nasal septum; pmx, premaxilla; ppmx, palatal process of maxilla; pppx, palatal process of premaxilla; ps, palatal shelf; t, tongue.

Loss of *Wnt9b* causes reduced outgrowth and contact failure of the NP and MxP

The upper lip in mice is formed by a coordinated outgrowth and fusion of the MxP of BA1 with the LNP and MNP by E11.5. To investigate whether developmental defects of these processes are

associated with CL/P in *Wnt9b*$^{-/-}$ mice, embryos were examined by scanning electron microscopy. No morphological defects were apparent in *Wnt9b*$^{-/-}$ embryos prior to E10.5. Reduced invagination of the nasal pit, especially near the posterior region, was seen at E10.5 (arrow in Fig. 2A,B; *n*=2). At E11, hypoplasia of the LNP and MNP became evident and the MNP failed to extend toward the LNP in *Wnt9b*$^{-/-}$ embryos, in contrast to wild-type embryos (Fig. 2C-F; *n*=2). Approximately half a day later in gestation, *Wnt9b*$^{-/-}$ embryos showed a clear bilateral gap between the MNP and the medial end of the fused LNP and MxP (Fig. 2G,H; *n*=2).

Reduced cell proliferation within the mesenchyme of the NP and MxP of *Wnt9b*$^{-/-}$ embryos

To investigate whether hypoplasia and failed fusion of the three processes are associated with specific cellular defects within the processes, we examined cell proliferation and apoptosis in *Wnt9b*$^{-/-}$ embryos. BrdU incorporation after pulse labeling and presence of phospho-histone H3, a marker for mitotic cells in G2/M phase, were used to assess cell proliferation. A significant reduction in the numbers of BrdU-positive and phospho-histone H3-positive cells was detected mainly in the mesenchymal compartment of both the NP and MxP of *Wnt9b*$^{-/-}$ embryos at E10.5 (Fig. 3).

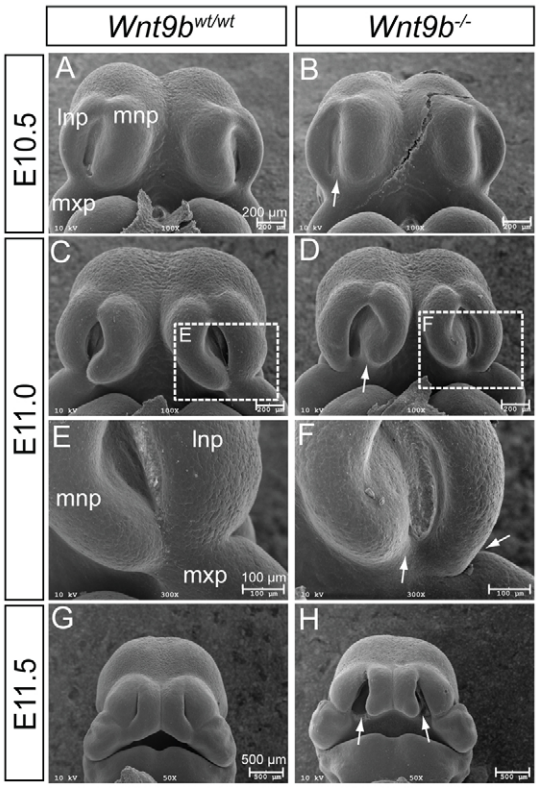

Fig. 2. Scanning electron microscopy analysis of facial development. (**A-H**) Front facial views of wild-type (A,C,E,G) and *Wnt9b*$^{-/-}$ (B,D,F,H) mouse embryos from E10.5 to E11.5. The boxed regions in C and D are magnified in E and F, respectively. Reduced invagination between the MNP and LNP was clear in *Wnt9b*$^{-/-}$ embryos at E10.5 (arrow in B). At E11.0, hypoplasia of the MNP and LNP was obvious, and the MNP, LNP and MxP failed to complete fusion (arrows in D,F). At E11.5, bilateral lip clefts (arrows in H) were apparent in *Wnt9b*$^{-/-}$ embryos. lnp, lateral nasal process; mnp, medial nasal process; mxp, maxillary process.

In wild-type embryos, cell apoptosis examined by activated caspase 3 (aCasp3) immunostaining and TUNEL assay appeared to be a rare event within the processes (supplementary material Fig. S3A). Apoptosis was detected in the epithelial seam in the fusion zone of the MNP, LNP and MxP of wild-type embryos at E10.5 (arrow in supplementary material Fig. S3A). By contrast, no apoptosis was observed in the posterior tips (prospective fusion zone) of the MNP and LNP in *Wnt9b*$^{-/-}$ embryos at E10.5 (supplementary material Fig. S3B). However, despite the failed contact and fusion, some apoptosis was observed in the end region of the MNP and LNP of *Wnt9b*$^{-/-}$ embryos at E11, suggesting delayed development of the NPs and MxP (data not shown). Comparable results were obtained by TUNEL labeling (data not shown).

We further determined whether fusion between the NP and MxP is defective in *Wnt9b*$^{-/-}$ embryos. The NP and MxP dissected from *Wnt9b*$^{-/-}$ embryos at E11-11.5 efficiently fused (*n*=7/7) in ex vivo facial explant culture (supplementary material Fig. S3C-E).

Taken together, these results indicate that CL/P in *Wnt9b*$^{-/-}$ mice is likely to be caused by retarded and/or delayed outgrowth and subsequent failure of physical contact of the NP and MxP, primarily owing to the cell proliferation defect of mesenchymal cells.

WNT9B specifically regulates canonical WNT/β-catenin signaling within the NP and MxP

WNT9B activates both WNT/β-catenin and WNT/planar cell polarity (PCP) signaling during kidney development (Carroll et al., 2005; Karner et al., 2011) and in HEK293T cells (data not shown). To determine whether ablation of *Wnt9b* attenuates WNT/β-catenin signaling within craniofacial structures, we examined expression of a WNT/β-catenin signaling reporter, *TopGAL*, in *Wnt9b*$^{-/-}$ embryos. At E10.5, *TopGAL* expression was significantly reduced in both surface ectodermal and underlying mesenchymal cells of the NPs and MxP in *Wnt9b*$^{-/-}$ mutants compared with wild-type embryos (black arrows in Fig. 4A-D), suggesting that *Wnt9b* expressed in ectoderm regulates WNT/β-catenin signaling in both ectodermal and mesenchymal cells of the NPs and MxP. Surprisingly, there was no reduction of *TopGAL* expression in the MdP of *Wnt9b*$^{-/-}$ embryos (white arrows in Fig. 4A,B), despite robust *Wnt9b* expression in the MdP ectoderm. This might explain why no mandible defect was observed in *Wnt9b*$^{-/-}$ mutants and also suggests that *Wnt9b* function in mandibular arch development is not essential, possibly being compensated by other WNT genes expressed in the MdP.

In addition, presence of the activated β-catenin protein, the phosphorylated LRP6 receptor and expression of *Axin2* were severely reduced in these facial processes of *Wnt9b*$^{-/-}$ embryos (Fig. 4E-G and Fig. 7I). Expression of the WNT/β-catenin signaling target genes *Msx1* and *Msx2* (Song et al., 2009), which are expressed in mesenchymal cells within the NPs and MxP (Gauchat et al., 2000; Alappat et al., 2003; Ishii et al., 2005), was also reduced in *Wnt9b*$^{-/-}$ embryos (Fig. 4H-K and Fig. 7I).

To confirm that *Wnt9b* function is associated with WNT/β-catenin signaling, we treated the NP/MxP explants isolated from *TopGAL* transgenic embryos with recombinant WNT9B protein. The WNT9B protein effectively increased *TopGAL* transgene expression in both whole (ectoderm/mesenchyme) and mesenchymal explants (Fig. 5A-D). In similar explant cultures, WNT9B robustly activated expression of the WNT/β-catenin signaling targets *Axin2*, *Msx1* and *Msx2* and inhibited *Raldh3* (*Aldh1a3* – Mouse Genome Informatics), which is negatively

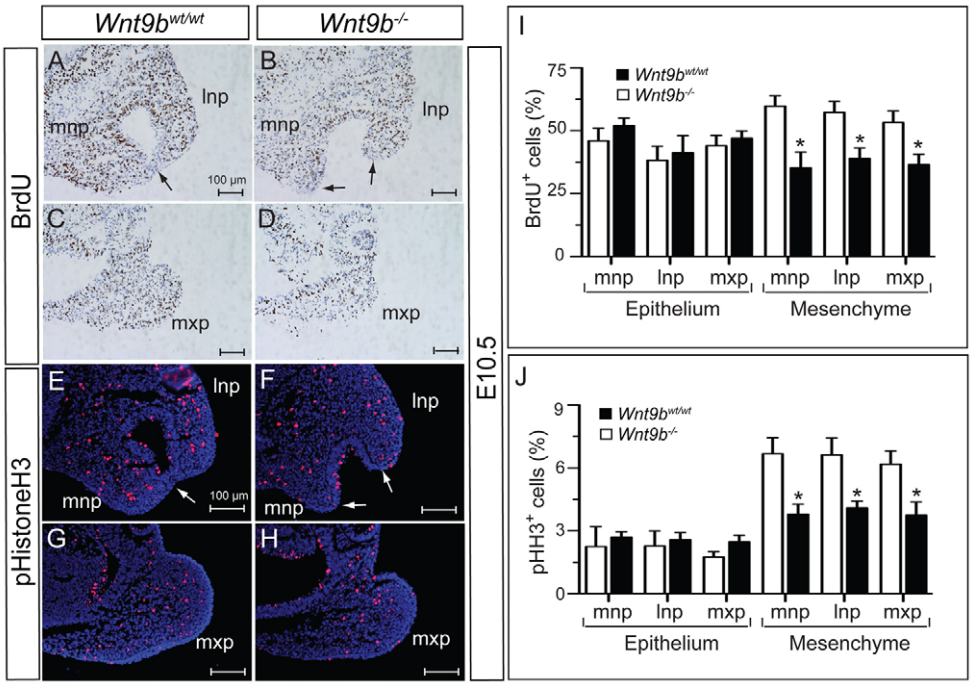

Fig. 3. Cell proliferation in the lip fusion zone. (**A-D**) Immunostaining for incorporated BrdU in the facial processes at E10.5. Note that the epithelial layer in the fusion area lacks BrdU-positive cells (arrows). (**E-H**) Mitotic cells detected by phospho-histone H3 in the facial processes at E10.5. The epithelial layer in the fusion area lacks phospho-histone H3-positive cells (arrows). (**I,J**) For calculating the proliferation rate, the numbers of BrdU-positive or phospho-histone H3-positive cells were counted in each of two sections of three embryos. Mean±s.e.m. **P*<0.05, Student's *t*-test. lnp, lateral nasal process; mnp, medial nasal process; mxp, maxillary process.

regulated by WNT/β-catenin signaling activity (Song et al., 2009) (Fig. 5E,F; supplementary material Fig. S4A). WNT9B also efficiently rescued the reduced *Axin2*, *Msx1* and *Msx2* expression in *Wnt9b*$^{-/-}$ explants (supplementary material Fig. S4A).

We next tested whether the defects associated with loss of *Wnt9b* are rescued in vivo by activation of β-catenin signaling. When LiCl, a GSK3β inhibitor that activates WNT/β-catenin signaling, was administered in utero, the elevated *Raldh3* expression in *Wnt9b*$^{-/-}$ embryos (Fig. 5G,H) was effectively reversed (Fig. 5I,J). This rescue effect was further confirmed in NP/MxP tissues isolated from embryos after in utero LiCl administration by qRT-PCR, as reduced expression of *Axin2*, *Msx1* and *Msx2* and increased expression of *Raldh3* in *Wnt9b*$^{-/-}$ embryos were reversed by LiCl (Fig. 5K). Taken together, these results confirmed that WNT/β-catenin signaling was severely compromised in the NPs and MxP of *Wnt9b*$^{-/-}$ embryos.

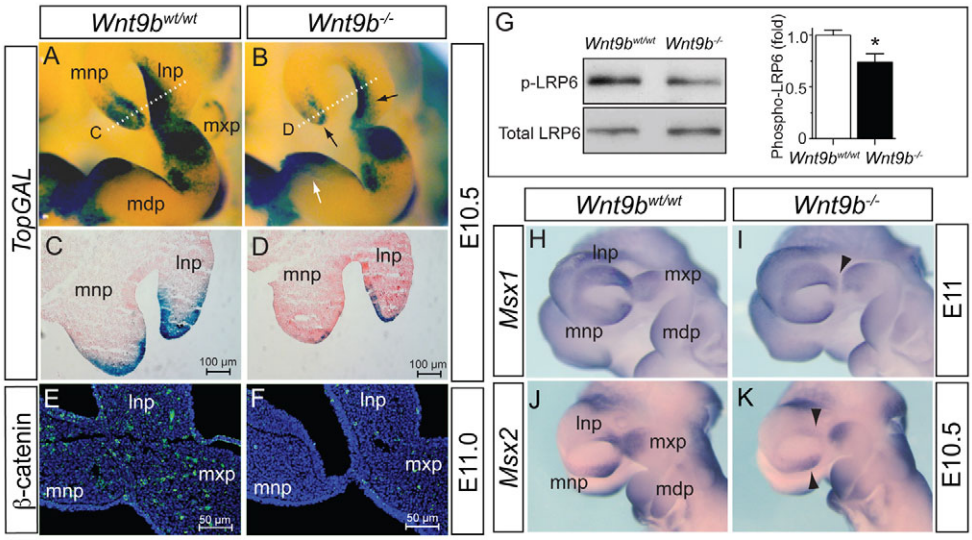

Fig. 4. Disruption of WNT/β-catenin signaling in *Wnt9b*$^{-/-}$ embryos. (**A-D**) *TopGAL* expression detected by colorimetric staining of β-galactosidase activity in wild-type and *Wnt9b*$^{-/-}$ mouse embryos. Black arrows indicate the NPs where significantly reduced *TopGAL* expression was observed in *Wnt9b*$^{-/-}$ embryos. There was no reduction of *TopGAL* expression in the MdP (white arrow in B). Dotted white lines in A and B indicate the plane of sections shown in C and D, respectively. Decreased *TopGAL* expression was apparent in both surface ectoderm and mesenchyme of the NPs (C,D). (**E**,**F**) Immunofluorescent staining of active β-catenin protein (green) in the facial processes at E11.0. (**G**) Western blot analysis of phosphorylated LRP6 in NP and MxP tissue lysates. Total LRP6 level provided a protein loading control. Signal levels from the triplicate samples were quantified using ImageJ and are presented as mean±s.e.m. **P*<0.05, Student's *t*-test. (**H-K**) *Msx1* and *Msx2* expression in E10.5-11 embryos was determined by whole-mount in situ hybridization. Arrowheads indicate the reduced expression domains in *Wnt9b*$^{-/-}$ embryos. mdp, mandibular process of branchial arch 1; lnp, lateral nasal process; mnp, medial nasal process; mxp, maxillary process.

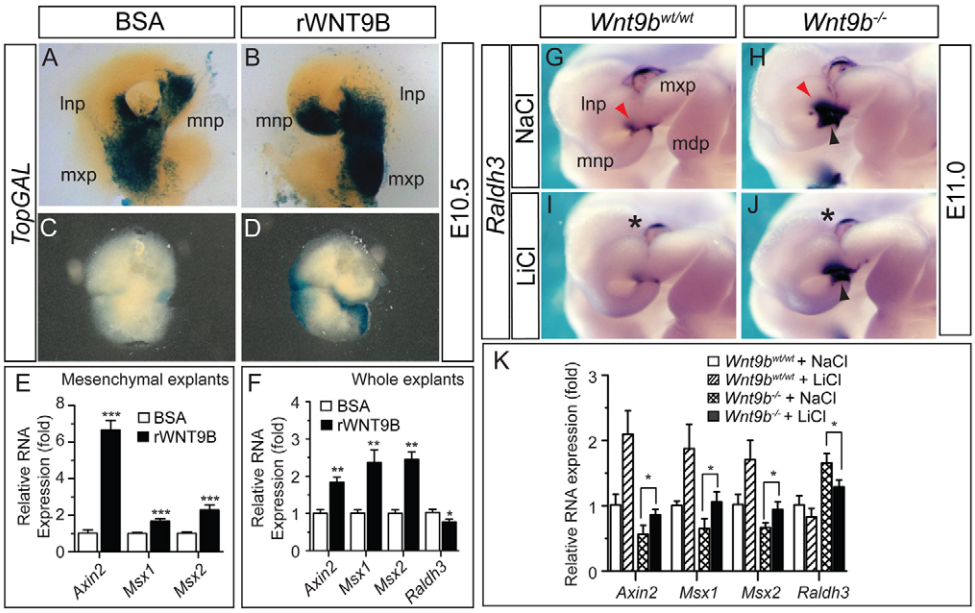

Fig. 5. Ex vivo activation of WNT/β-catenin signaling in the NP and MxP by WNT9B protein and in vivo activation of WNT/β-catenin signaling by LiCl in *Wnt9b*$^{-/-}$ embryos. (**A-D**) Ex vivo facial explant culture. A pair of NP/MxP explants was dissected from the same *TopGAL* mouse embryo at E10.5 and cultured in the absence or presence of recombinant WNT9B protein (800 ng/ml) for up to 36 hours. Either whole (ectoderm plus mesenchyme, A,B) or mesenchyme (C,D) explants were cultured and stained for β-galactosidase activity. (**E**,**F**) qRT-PCR analysis of gene expression in the NP/MxP explants cultured in the absence or presence of WNT9B. The relative expression level compared with the BSA-treated control samples is presented as mean±s.e.m. **P*<0.05, ***P*<0.01, ****P*<0.005, Student's *t*-test. (**G-J**) Elevated *Raldh3* expression in the facial processes of *Wnt9b*$^{-/-}$ embryos at E10.5 was repressed by in utero LiCl administration. Red arrowheads (G,H) indicate elevated *Raldh3* expression in *Wnt9b*$^{-/-}$ embryos, whereas black arrowheads (I,J) indicate suppression of the elevated *Raldh3* expression by LiCl. *Wnt9b*-independent *Raldh3* expression in the developing eye is indicated by asterisks. (**K**) Quantitative expression analysis of other WNT targets and *Raldh3* in *Wnt9b*$^{-/-}$ embryos after in utero LiCl administration. Total RNAs were isolated from the dissected NP and MxP tissues. Mean±s.e.m. **P*<0.05, Student's *t*-test. mdp, mandibular process of branchial arch 1; lnp, lateral nasal process; mnp, medial nasal process; mxp, maxillary process.

Deletion of *Wnt9b* has no obvious effect on WNT/PCP signaling

To determine whether loss of *Wnt9b* influences non-canonical WNT/PCP signaling activity, we examined activation of RHOA, RAC1 and CDC42, three small GTPases key to the WNT/PCP pathway, in tissue lysates prepared from the NP and MxP of E10.5 embryos. No differences in the activation of these proteins were observed between *Wnt9b*$^{-/-}$ and wild-type embryos (Fig. 6A). We also found no significant differences in the levels of phosphorylated JNK1/2 (MAPK8/9 – Mouse Genome Informatics) and ROCK2, two kinases activated by RHOA/RAC1/CDC42, between *Wnt9b*$^{-/-}$ and wild-type embryos (Fig. 6B). Finally, immunostaining of phosphorylated c-JUN, a target for activated JNK, did not show any differences between wild-type and *Wnt9b*$^{-/-}$ embryos, except in the fusion zone of the MNP and LNP (Fig. 6C,D). This phosphorylation of c-JUN is likely to be associated with cell apoptosis in wild-type embryos (supplementary material Fig. S3A,B) (Jiang et al., 2006) but not with non-canonical WNT/PCP signaling. Therefore, we conclude that unlike kidney development, loss of *Wnt9b* has no apparent effect on non-canonical WNT/PCP signaling during facial development.

WNT9B regulates FGF family gene expression within the ectoderm of the NP and MxP

It is well known that ectoderm-derived signals such as FGF, BMP and SHH regulate mesenchymal cell proliferation/survival and differentiation in the facial processes (Abu-Issa et al., 2002; Liu et al., 2005; Alkuraya et al., 2006; Riley et al., 2007). We found that there was significant downregulation of several FGF family genes within the facial processes in *Wnt9b*$^{-/-}$ embryos at E10.5-11 (Fig. 7), whereas *Bmp4* and *Shh* expression was not modified (supplementary material Fig. S5). Expression of *Fgf8*, *Fgf10* and *Fgf17* was either absent or severely reduced in the LNP and MNP at E10.5 (Fig. 7A-I). Additionally, *Fgf8* and *Fgf10* expression remained reduced in the NPs of *Wnt9b*$^{-/-}$ embryos at E11 (Fig. 7C,D; data not shown).

To determine whether these FGF genes are regulated by WNT/β-catenin signaling activated by WNT9B, we examined their expression in the NP/MxP explants treated with WNT9B protein. WNT9B significantly induced the expression of three FGF genes in wild-type explants and effectively reversed the reduced FGF gene expression in *Wnt9b*$^{-/-}$ explants (supplementary material Fig. S4A). Consistent with these results, reduced FGF gene expression in *Wnt9b*$^{-/-}$ embryos was efficiently reversed by in utero treatment with LiCl (supplementary material Fig. S4B). We next examined FGF gene expression in E10.5 embryos in which β-catenin is constitutively activated within the ectoderm of the NP and MxP by *Foxg1-Cre*-mediated recombination of the *Ctnnb1*$^{+/loxp(Ex3)}$ allele (Harada et al., 1999). All three FGF genes, as well as *Axin2*, were highly induced by activated β-catenin, whereas *Raldh3* expression decreased (Fig. 7J).

Ectodermal FGFs induced by *Wnt9b* regulate proliferation of facial process mesenchymal cells

To determine whether reduced ectodermal FGF gene expression resulted in a decrease in FGF signaling in the facial processes, we examined phosphorylation of ERK1/2 (MAPK3/1 – Mouse

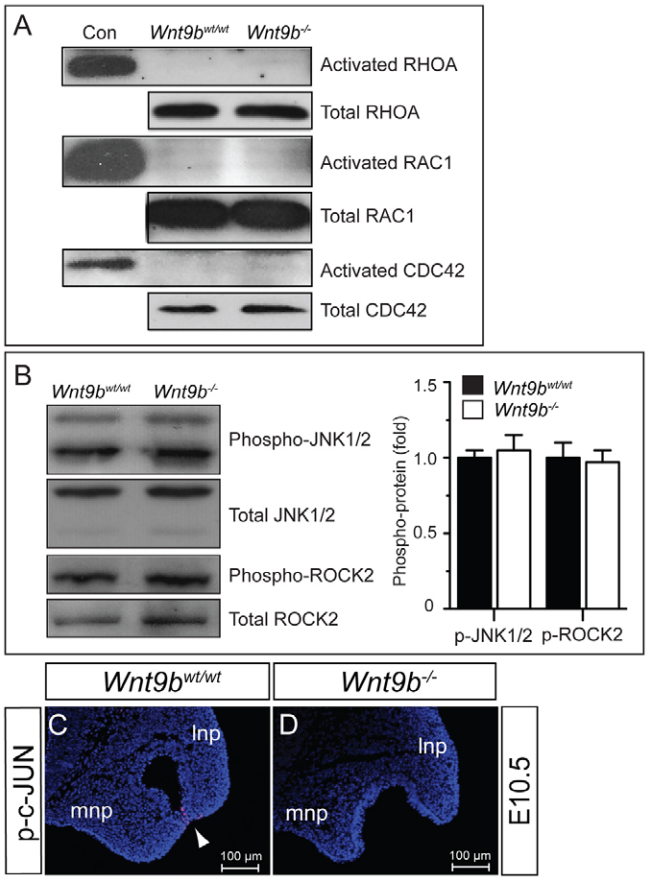

Fig. 6. *Wnt9b*$^{-/-}$ embryos exhibit no significant change in WNT/PCP signaling in the facial processes. (**A**) Western blot analysis of activated RHOA, RAC1 and CDC42 small GTPases. No significant changes in these GTPase activities were detected in the NP/MxP tissue lysates isolated from E10.5 *Wnt9b*$^{-/-}$ mouse embryos compared with those of wild-type embryos. The levels of total RHOA, RAC1 and CDC42 proteins were also determined as protein controls. (**B**) Western blot analysis of JNK1/2 and ROCK2 activation. Protein lysates prepared from the NP/MxP tissues of wild-type and *Wnt9b*$^{-/-}$ embryos at E10.5 were analyzed for phospho-JNK1/2 and phospho-ROCK2. Total JNK1/2 and ROCK2 levels were measured for loading control. Using ImageJ, signal levels were quantified from triplicate samples and are presented as mean±s.e.m. (**C**,**D**) Immunofluorescence staining of phosphorylated c-JUN in the MNP and LNP. No overt staining was detected in the NPs of either wild-type or *Wnt9b*$^{-/-}$ embryos at E10.5. A positive signal (red) was detected only in epithelial cells within the fusion zone in wild-type embryos (arrowhead).

Genome Informatics), a signature downstream event in FGF signaling. A significant reduction of phosphorylated ERK1/2-positive cells was observed in the NP and MxP of *Wnt9b*$^{-/-}$ embryos at E10.5, which was especially evident within the mesenchymal compartment of the NP (Fig. 8A-C).

To determine whether ERK1/2 activation in facial process mesenchymal cells is primarily mediated by ectodermal FGFs induced by *Wnt9b*, we examined ERK1/2 phosphorylation in facial process mesenchymal cells treated with FGF and WNT9B proteins. Both FGF8 and FGF10 effectively phosphorylated ERK1/2 within 15 minutes of treatment, and this phosphorylation was reversed in the presence of a specific FGFR inhibitor, NP603 (Kammasud et al., 2007) (Fig. 8D). By contrast, WNT9B was unable to induce phosphorylation of ERK1/2 in these cells.

We next investigated whether WNT9B and FGFs are mitogenic for facial process mesenchymal cells. WNT9B treatment did not enhance the proliferation of mesenchymal cells isolated from the NP and MxP of E10.5 embryos (Fig. 8E). By contrast, both FGF8 and FGF10 efficiently enhanced proliferation of these cells (Fig. 8F). Furthermore, proliferation of mesenchymal cells prepared from *Wnt9b*$^{-/-}$ embryos was also enhanced by FGFs to a level comparable to wild-type cells (Fig. 8F).

We also examined whether the FGF and WNT9B proteins have any effect on mesenchymal cell migration. The migratory behavior of mesenchymal cells in wound-healing and Transwell cell migration assays were unaffected by FGF or WNT9B (supplementary material Fig. S6).

Taken together, we conclude that WNT9B positively regulates FGF gene expression in the ectoderm of the NP and MxP, and that WNT9B-induced ectodermal FGF signaling is required for the proliferation of mesenchymal cells within the NPs and MxP (Fig. 8G).

DISCUSSION

Wnt9b controls outgrowth of facial processes through the canonical WNT/β-catenin pathway

The primary embryonic defect of facial development in *Wnt9b*$^{-/-}$ mutants is hypoplasia with reduced outgrowth of the NPs and MxP (Fig. 2) as a direct consequence of reduced proliferation (Fig. 3). A subsequent failure of physical contact between the LNP and MNP at ~E10-11.5 prevents fusion between the facial processes (Fig. 2) and eventually results in cleft lip with cleft palate at later stages in *Wnt9b*$^{-/-}$ mice (Fig. 1). Several lines of evidence confirm that these cellular defects result from compromised WNT/β-catenin signaling. A significant reduction in active β-catenin protein accumulation, in phosphorylation of the LRP6 receptor and in expression of WNT/β-catenin signaling reporter and downstream target genes in the NP and MxP were observed in *Wnt9b*$^{-/-}$ embryos (Figs 4, 5). The recombinant WNT9B protein effectively increased WNT/β-catenin signaling in facial process explant cultures in vitro (Fig. 5). Furthermore, in utero LiCl treatment partially restored β-catenin activation in *Wnt9b* null embryos as assessed by target gene expression at E10.5-11 (Fig. 5G-K; supplementary material Fig. S4B). However, morphological defects, when observed in E13.5 embryos, were not rescued by in utero LiCl administration (data not shown), suggesting that the LiCl administration scheme (timing, dosage and frequency) might not be optimal for phenotypic rescue. Additionally, because GSK3β also plays a key role in the negative regulation of SHH signaling through the phosphorylation of the GLI2/3 transcription factors (Lum and Beachy, 2004), in utero LiCl treatment can activate SHH signaling simultaneously. A genetic approach to WNT signaling activation or the use of a more specific WNT signaling activator is warranted to determine whether the defects in *Wnt9b*$^{-/-}$ embryos can be rescued by activation of β-catenin signaling.

Consistent with the phenotypes of *Wnt9b* mutants, *Lrp6* mutant mice show a full penetrance of CL/P with retarded outgrowth of the NP and MxP (Song et al., 2009). In these mutant mice, severely reduced proliferation without apparent apoptosis is evident in mesenchymal cells of the NP and MxP (Song et al., 2009). Moreover, WNT9B protein has been shown to directly bind to the extracellular domain of the LRP6 receptor using an in vitro protein interaction assay (Bourhis et al., 2010; Gong et al., 2010), strongly suggesting that WNT9B transmits its signal through the LRP6 receptor in the facial processes.

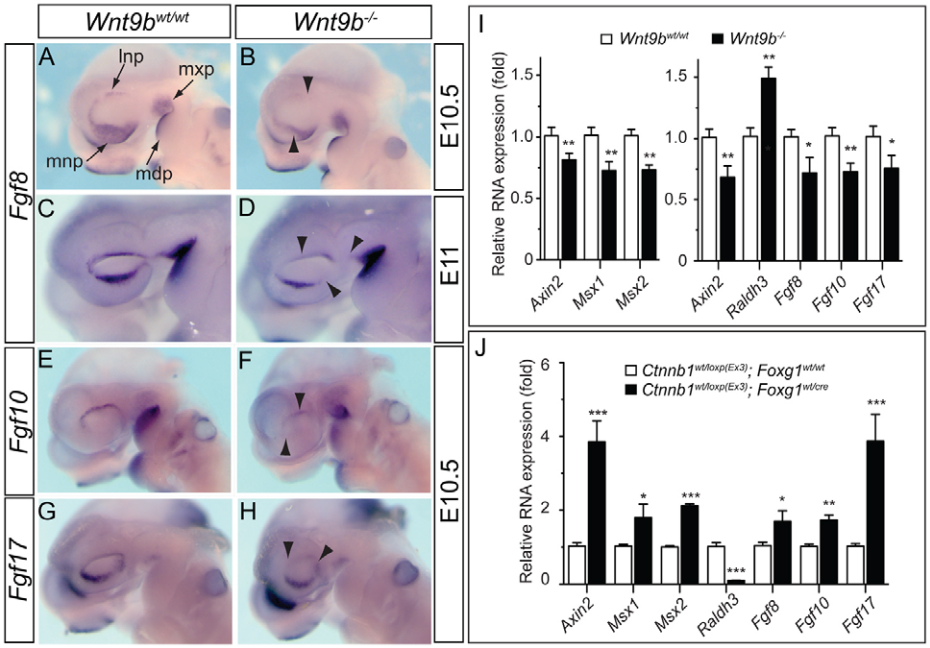

Fig. 7. FGF family gene expression in the facial processes of E10.5 and E11 embryos. (**A-H**) *Fgf8* (A-D), *Fgf10* (E,F) and *Fgf17* (G,H) expression was significantly reduced (arrowheads) in the MNP and LNP of *Wnt9b*$^{-/-}$ mouse embryos at E10.5. *Fgf8* expression remained reduced at E11. (**I**) Quantitative analysis of gene expression in the dissected NP/MxP tissues of wild-type and *Wnt9b*$^{-/-}$ mutants at E10.5. The NP/MxP tissues containing both ectoderm and mesenchyme (right bar chart) and ectoderm separated from mesenchyme (left bar chart) were analyzed. (**J**) Gene expression in the upper facial processes of embryos in which *Ctnnb1* function was constitutively activated in the facial ectoderm. The relative expression level compared with wild-type samples is presented as mean±s.e.m. **P*<0.05, ***P*<0.01, ****P*<0.005, Student's *t*-test. mdp, mandibular process of branchial arch 1; lnp, lateral nasal process; mnp, medial nasal process; mxp, maxillary process.

Ectoderm-specific inactivation and activation of *Ctnnb1* in the facial processes caused severe hypoplasia and hyperplasia of the facial processes, respectively (Reid et al., 2011; Wang et al., 2011). Mesenchyme-specific *Ctnnb1* deletion in the facial processes also causes severe defects in facial development, with missing facial skeletal components accompanying significant hypoplasia in the frontofacial region and BA1 (Brault et al., 2001). Interestingly, unlike *Wnt9b* and *Lrp6* mutants, increased apoptosis without reduced proliferation was detected in both ectodermal and mesenchymal cells of the BA1 and NPs of *Ctnnb1* deletion mutants (Brault et al., 2001; Wang et al., 2011). Inactivation of *Wnt9b* or *Lrp6* might only partially remove the activity of WNT/β-catenin signaling in the facial processes, as *Lrp5* and other WNT genes can provide the remaining WNT signaling activity. Different cellular defects (proliferation versus apoptosis) observed in mice lacking *Ctnnb1*, *Lrp6* or *Wnt9b* also strongly suggest that multiple cellular processes are regulated by WNT/β-catenin signaling within the facial processes.

WNT9B cannot activate non-canonical WNT/PCP signaling during facial development

A previous study demonstrated that *Wnt9b* also acts through the non-canonical WNT/PCP pathway, mainly the RHOA-JNK signaling cascade, during kidney development (Karner et al., 2009). In contrast to kidney development, we failed to detect any indication of reduced (or induced) WNT/PCP signaling in the facial processes of *Wnt9b*$^{-/-}$ embryos (Fig. 6). In general, there is scant WNT/PCP signaling activity within these processes in wild-type embryos.

Consistent with this notion, ectoderm- and mesenchyme-specific deletion of *Rac1*, *Cdc42* or *RhoA* in the facial processes does not result in any notable phenotypic defects in facial structures until E10.5 (Chen et al., 2006; Fuchs et al., 2009; Thomas et al., 2010; Katayama et al., 2011). No morphological hypoplasia was found in the NP and MxP of mesenchyme-specific *Rac1* and *Cdc42* mutant mice at E11 (Fuchs et al., 2009; Thomas et al., 2010). Severe malformations of neural crest-derived structures and mid-facial cleft appeared in these mutants at ~E11.5.

Mice lacking both the *Fzd1* and *Fzd2* receptor genes exhibit signatures of defective WNT/PCP signaling, including a failure of closure in the palate, ventricular septum and neural tube, and misorientation of inner ear sensory hair cells (Yu et al., 2010). However, these mice still display normal development of the NP and MxP and lip fusion. Taken together, our results and previously published reports suggest that non-canonical WNT/PCP signaling plays insignificant or minimal roles within the NPs and MxP during the stage when the defects associated with *Wnt9b* null mutation are apparent.

WNT/β-catenin signaling is required for FGF gene expression in facial process ectoderm to induce mesenchyme cell proliferation

Reduced cell proliferation in mesenchymal cells of the facial processes in *Wnt9b*$^{-/-}$ embryos raises the question of whether ectoderm-derived WNT9B ligand can act as a mitogen for mesenchymal cells. The recombinant WNT9B protein failed to induce proliferation of primary facial mesenchyme cells in culture (Fig. 8), arguing that WNT9B might not be a mitogen that induces mesenchyme cell proliferation. Given the evident reduction of WNT/β-catenin signaling activity within the ectodermal layer of the NP and MxP in *Wnt9b* mutants, it is plausible that WNT9B might induce ectoderm-derived mitogens.

It is known that FGF signaling plays crucial roles in facial development. Among 22 FGF genes, at least seven (*Fgf3*, *Fgf8*, *Fgf9*, *Fgf10*, *Fgf15*, *Fgf17* and *Fgf18*) are expressed with a regional specificity within the ectoderm of the facial processes in mice between E9.5 and E10.5 (Bachler and Neubuser, 2001). We found that *Fgf8*, *Fgf10* and *Fgf17* RNA expression and FGF-induced phosphorylation of ERK1/2 were significantly reduced in the NP and MxP of *Wnt9b*$^{-/-}$ embryos (Figs 7, 8). Ectoderm-specific activation of β-catenin in the facial processes resulted in increased expression of these FGF genes (Fig. 7M), strongly suggesting that they are targets for WNT/β-catenin signaling. Indeed, *Fgf8* and *Fgf10* were previously identified as direct WNT/β-catenin target genes in facial and cardiac tissues, respectively (Cohen et al., 2007; Wang et al., 2011).

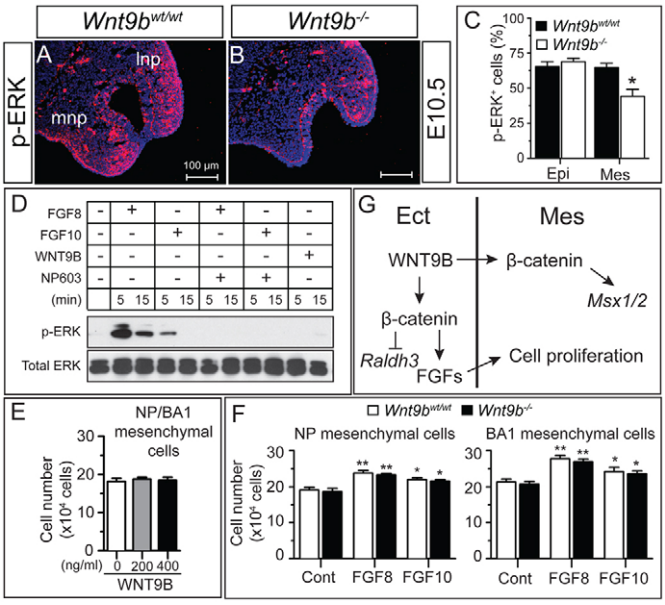

Fig. 8. Increased cell proliferation and ERK1/2 phosphorylation by FGFs in facial process mesenchymal cells. (**A-C**) Reduced ERK1/2 phosphorylation in the NP of *Wnt9b*$^{-/-}$ mouse embryos. Immunostained images (A,B) and their quantitation (C) are presented. (**D**) Activation of ERK1/2 phosphorylation by FGF8 and FGF10. The upper facial mesenchymal cells were stimulated with FGFs or WNT9B for 5 or 15 minutes. NP603 (5 μM) was added to the cells simultaneously with FGFs. Total and phosphorylated ERK1/2 protein levels were analyzed by western blot. (**E**,**F**) Mesenchymal cell proliferation was enhanced by FGF8 and FGF10 but not WNT9B. Mesenchymal cells isolated from the wild-type or *Wnt9b*$^{-/-}$ NP/MxP explants were cultured in the presence of FGFs or WNT9B for 3 days. Total cell numbers were counted. Mean±s.e.m. **P*<0.05, ***P*<0.01, Student's *t*-test. (**G**) Model for WNT9B function in upper facial development. The facial ectoderm-derived WNT9B regulates the FGF family genes and *Raldh3* in ectoderm and the *Msx1/2* genes in mesenchyme in a β-catenin-dependent manner. Cell proliferation within mesenchyme is directly regulated by WNT9B-induced FGFs. Epi, epithelium; Ect, surface ectoderm; Mes, mesenchyme; lnp, lateral nasal process; mnp, medial nasal process.

The cellular consequence of reduced FGF signaling in the facial processes in mice deficient of WNT/β-catenin signaling remains unclear. BA1 ectoderm-specific *Fgf8* deletion studies have shown that ectodermal FGF signaling is mainly required for mesenchymal cell survival in BA1 (Trumpp et al., 1999), whereas reduced cell proliferation is a major response affected by reduced FGF signaling in the NP and MxP of *Lrp6* (Song et al., 2009) and *Wnt9b* (this study) mutant mice. There are several possible explanations for these seemingly contradictory results. One possibility is that ectoderm-derived FGF signaling plays roles in both the survival and proliferation of mesenchyme cells in the facial processes in a concentration-dependent manner. For instance, cell survival might require low-level FGF signaling, whereas cell proliferation might need higher levels of FGF signaling and be more sensitive to the reduced FGF signaling. It is noteworthy that FGF2 differentially regulates the behavior of cranial neural crest cells in a dose-dependent manner in vitro, enhancing proliferation at lower doses and inducing differentiation at higher doses (Sarkar et al., 2001). In embryos carrying an ectoderm-specific *Ctnnb1* deletion, in which canonical WNT signaling is almost completely blocked, more severe downregulation of FGF gene expression and increased cell apoptosis were observed (Reid et al., 2011; Wang et al., 2011). By contrast, because loss of *Wnt9b* or *Lrp6* partially reduces FGF gene expression, the residual FGFs might protect cells from death but not support efficient cell proliferation.

Another possibility is a differential tissue response to FGFs. FGF signaling primarily controls cell survival in the MdP and telencephalon (Trumpp et al., 1999; Paek et al., 2009; Paek et al., 2011). Ablation of *Ctnnb1* in the facial ectoderm induces more significant cell death in BA1 than in the NPs (Reid et al., 2011), suggesting that there might be a differential response to FGF signaling in these cells. These observations, including our present findings, suggest the interesting possibility that fine-tuned FGF signaling activity differentially regulates two distinct cellular behaviors, i.e. proliferation and survival, within the facial processes.

Acknowledgements
We thank Drs Thomas Gridley, Jin-Seon Lee, Lucy Liaw and Doug Spicer for comments and suggestions; Norma Albrecht for proofreading the manuscript; and Drs Thomas Carroll and Terry Yamaguchi for providing mouse lines.

Funding
This research was supported by National Institutes of Health grants from the National Institute of Arthritis and Musculoskeletal and Skin Diseases (NIAMS) [5R01 AR055278 to J.K.Y.] and the National Institute of General Medical Sciences (NIGMS) [8P20 GM103465 to J.K.Y.] (Program Director D. Wojchowski). The core facilities that support this work were funded by NIGMS [Histopathology and Bioinformatics cores, 8P20 GM103465 to D. Wojchowski; Mouse Transgenic, Histopathology and DNA Analysis cores, 8P30 GM103392 to R. Friesel]. Deposited in PMC for release after 12 months.

Competing interests statement
The authors declare no competing financial interests.

Supplementary material
Supplementary material available online at
http://dev.biologists.org/lookup/suppl/doi:10.1242/dev.075796/-/DC1

References

Abu-Issa, R., Smyth, G., Smoak, I., Yamamura, K. and Meyers, E. N. (2002). Fgf8 is required for pharyngeal arch and cardiovascular development in the mouse. *Development* **129**, 4613-4625.
Al Alam, D., Green, M., Tabatabai Irani, R., Parsa, S., Danopoulos, S., Sala, F. G., Branch, J., El Agha, E., Tiozzo, C., Voswinckel, R. et al. (2011). Contrasting expression of canonical wnt signaling reporters TOPGAL, BATGAL and Axin2 during murine lung development and repair. *PLoS ONE* **6**, e23139.
Alappat, S., Zhang, Z. Y. and Chen, Y. P. (2003). Msx homeobox gene family and craniofacial development. *Cell Res.* **13**, 429-442.
Alkuraya, F. S., Saadi, I., Lund, J. J., Turbe-Doan, A., Morton, C. C. and Maas, R. L. (2006). SUMO1 haploinsufficiency leads to cleft lip and palate. *Science* **313**, 1751.
Bachler, M. and Neubuser, A. (2001). Expression of members of the Fgf family and their receptors during midfacial development. *Mech. Dev.* **100**, 313-316.
Bourhis, E., Tam, C., Franke, Y., Bazan, J. F., Ernst, J., Hwang, J., Costa, M., Cochran, A. G. and Hannoush, R. N. (2010). Reconstitution of a frizzled8.Wnt3a.LRP6 signaling complex reveals multiple Wnt and Dkk1 binding sites on LRP6. *J. Biol. Chem.* **285**, 9172-9179.
Brault, V., Moore, R., Kutsch, S., Ishibashi, M., Rowitch, D. H., McMahon, A. P., Sommer, L., Boussadia, O. and Kemler, R. (2001). Inactivation of the beta-catenin gene by Wnt1-Cre-mediated deletion results in dramatic brain malformation and failure of craniofacial development. *Development* **128**, 1253-1264.
Brugmann, S. A., Goodnough, L. H., Gregorieff, A., Leucht, P., ten Berge, D., Fuerer, C., Clevers, H., Nusse, R. and Helms, J. A. (2007). Wnt signaling mediates regional specification in the vertebrate face. *Development* **134**, 3283-3295.
Carroll, T. J., Park, J. S., Hayashi, S., Majumdar, A. and McMahon, A. P. (2005). Wnt9b plays a central role in the regulation of mesenchymal to epithelial transitions underlying organogenesis of the mammalian urogenital system. *Dev. Cell* **9**, 283-292.
Chen, L., Liao, G., Yang, L., Campbell, K., Nakafuku, M., Kuan, C. Y. and Zheng, Y. (2006). Cdc42 deficiency causes Sonic hedgehog-independent holoprosencephaly. *Proc. Natl. Acad. Sci. USA* **103**, 16520-16525.

Cohen, E. D., Wang, Z., Lepore, J. J., Lu, M. M., Taketo, M. M., Epstein, D. J. and Morrisey, E. E. (2007). Wnt/beta-catenin signaling promotes expansion of Isl-1-positive cardiac progenitor cells through regulation of FGF signaling. *J. Clin. Invest.* **117**, 1794-1804.
Creuzet, S., Couly, G. and Le Douarin, N. M. (2005). Patterning the neural crest derivatives during development of the vertebrate head: insights from avian studies. *J. Anat.* **207**, 447-459.
DasGupta, R. and Fuchs, E. (1999). Multiple roles for activated LEF/TCF transcription complexes during hair follicle development and differentiation. *Development* **126**, 4557-4568.
Dixon, M. J., Marazita, M. L., Beaty, T. H. and Murray, J. C. (2011). Cleft lip and palate: understanding genetic and environmental influences. *Nat. Rev. Genet.* **12**, 167-178.
Dunty, W. C., Jr, Biris, K. K., Chalamalasetty, R. B., Taketo, M. M., Lewandoski, M. and Yamaguchi, T. P. (2008). Wnt3a/beta-catenin signaling controls posterior body development by coordinating mesoderm formation and segmentation. *Development* **135**, 85-94.
Fuchs, S., Herzog, D., Sumara, G., Buchmann-Moller, S., Civenni, G., Wu, X., Chrostek-Grashoff, A., Suter, U., Ricci, R., Relvas, J. B. et al. (2009). Stage-specific control of neural crest stem cell proliferation by the small Rho GTPases Cdc42 and Rac1. *Cell Stem Cell* **4**, 236-247.
Gauchat, D., Mazet, F., Berney, C., Schummer, M., Kreger, S., Pawlowski, J. and Galliot, B. (2000). Evolution of Antp-class genes and differential expression of Hydra Hox/paraHox genes in anterior patterning. *Proc. Natl. Acad. Sci. USA* **97**, 4493-4498.
Geetha-Loganathan, P., Nimmagadda, S., Antoni, L., Fu, K., Whiting, C. J., Francis-West, P. and Richman, J. M. (2009). Expression of WNT signalling pathway genes during chicken craniofacial development. *Dev. Dyn.* **238**, 1150-1165.
Gong, Y., Bourhis, E., Chiu, C., Stawicki, S., DeAlmeida, V. I., Liu, B. Y., Phamluong, K., Cao, T. C., Carano, R. A., Ernst, J. A. et al. (2010). Wnt isoform-specific interactions with coreceptor specify inhibition or potentiation of signaling by LRP6 antibodies. *PLoS ONE* **5**, e12682.
Harada, N., Tamai, Y., Ishikawa, T., Sauer, B., Takaku, K., Oshima, M. and Taketo, M. M. (1999). Intestinal polyposis in mice with a dominant stable mutation of the beta-catenin gene. *EMBO J.* **18**, 5931-5942.
He, F., Xiong, W., Wang, Y., Li, L., Liu, C., Yamagami, T., Taketo, M. M., Zhou, C. and Chen, Y. (2011). Epithelial Wnt/beta-catenin signaling regulates palatal shelf fusion through regulation of Tgfbeta3 expression. *Dev. Biol.* **350**, 511-519.
Hebert, J. M. and McConnell, S. K. (2000). Targeting of cre to the Foxg1 (BF-1) locus mediates loxP recombination in the telencephalon and other developing head structures. *Dev. Biol.* **222**, 296-306.
Ishii, M., Han, J., Yen, H. Y., Sucov, H. M., Chai, Y. and Maxson, R. E., Jr (2005). Combined deficiencies of Msx1 and Msx2 cause impaired patterning and survival of the cranial neural crest. *Development* **132**, 4937-4950.
Jiang, R., Bush, J. O. and Lidral, A. C. (2006). Development of the upper lip: morphogenetic and molecular mechanisms. *Dev. Dyn.* **235**, 1152-1166.
Jin, Y. R., Turcotte, T. J., Crocker, A. L., Han, X. H. and Yoon, J. K. (2011). The canonical Wnt signaling activator, R-spondin2, regulates craniofacial patterning and morphogenesis within the branchial arch through ectodermal-mesenchymal interaction. *Dev. Biol.* **352**, 1-13.
Juriloff, D. M., Harris, M. J., Dewell, S. L., Brown, C. J., Mager, D. L., Gagnier, L. and Mah, D. G. (2005). Investigations of the genomic region that contains the clf1 mutation, a causal gene in multifactorial cleft lip and palate in mice. *Birth Defects Res. A Clin. Mol. Teratol.* **73**, 103-113.
Juriloff, D. M., Harris, M. J., McMahon, A. P., Carroll, T. J. and Lidral, A. C. (2006). Wnt9b is the mutated gene involved in multifactorial nonsyndromic cleft lip with or without cleft palate in A/WySn mice, as confirmed by a genetic complementation test. *Birth Defects Res. A Clin. Mol. Teratol.* **76**, 574-579.
Kammasud, N., Boonyarat, C., Tsunoda, S., Sakurai, H., Saiki, I., Grierson, D. S. and Vajragupta, O. (2007). Novel inhibitor for fibroblast growth factor receptor tyrosine kinase. *Bioorg. Med. Chem. Lett.* **17**, 4812-4818.
Karner, C. M., Chirumamilla, R., Aoki, S., Igarashi, P., Wallingford, J. B. and Carroll, T. J. (2009). Wnt9b signaling regulates planar cell polarity and kidney tubule morphogenesis. *Nat. Genet.* **41**, 793-799.
Karner, C. M., Das, A., Ma, Z., Self, M., Chen, C., Lum, L., Oliver, G. and Carroll, T. J. (2011). Canonical Wnt9b signaling balances progenitor cell expansion and differentiation during kidney development. *Development* **138**, 1247-1257.
Katayama, K., Melendez, J., Baumann, J. M., Leslie, J. R., Chauhan, B. K., Nemkul, N., Lang, R. A., Kuan, C. Y., Zheng, Y. and Yoshida, Y. (2011). Loss of RhoA in neural progenitor cells causes the disruption of adherens junctions and hyperproliferation. *Proc. Natl. Acad. Sci. USA* **108**, 7607-7612.
Kontges, G. and Lumsden, A. (1996). Rhombencephalic neural crest segmentation is preserved throughout craniofacial ontogeny. *Development* **122**, 3229-3242.
Lan, Y., Ryan, R. C., Zhang, Z., Bullard, S. A., Bush, J. O., Maltby, K. M., Lidral, A. C. and Jiang, R. (2006). Expression of Wnt9b and activation of canonical Wnt signaling during midfacial morphogenesis in mice. *Dev. Dyn.* **235**, 1448-1454.
Liu, W., Sun, X., Braut, A., Mishina, Y., Behringer, R. R., Mina, M. and Martin, J. F. (2005). Distinct functions for Bmp signaling in lip and palate fusion in mice. *Development* **132**, 1453-1461.
Lum, L. and Beachy, P. A. (2004). The Hedgehog response network: sensors, switches, and routers. *Science* **304**, 1755-1759.
Maretto, S., Cordenonsi, M., Dupont, S., Braghetta, P., Broccoli, V., Hassan, A. B., Volpin, D., Bressan, G. M. and Piccolo, S. (2003). Mapping Wnt/beta-catenin signaling during mouse development and in colorectal tumors. *Proc. Natl. Acad. Sci. USA* **100**, 3299-3304.
Menezes, R., Letra, A., Kim, A. H., Kuchler, E. C., Day, A., Tannure, P. N., Gomes da Motta, L., Paiva, K. B., Granjeiro, J. M. and Vieira, A. R. (2010). Studies with Wnt genes and nonsyndromic cleft lip and palate. *Birth Defects Res. A Clin. Mol. Teratol.* **88**, 995-1000.
Minoux, M. and Rijli, F. M. (2010). Molecular mechanisms of cranial neural crest cell migration and patterning in craniofacial development. *Development* **137**, 2605-2621.
Nagy, A., Moens, C., Ivanyi, E., Pawling, J., Gertsenstein, M., Hadjantonakis, A. K., Pirity, M. and Rossant, J. (1998). Dissecting the role of N-myc in development using a single targeting vector to generate a series of alleles. *Curr. Biol.* **8**, 661-664.
Niemann, S., Zhao, C., Pascu, F., Stahl, U., Aulepp, U., Niswander, L., Weber, J. L. and Muller, U. (2004). Homozygous WNT3 mutation causes tetra-amelia in a large consanguineous family. *Am. J. Hum. Genet.* **74**, 558-563.
Osumi-Yamashita, N., Ninomiya, Y., Doi, H. and Eto, K. (1994). The contribution of both forebrain and midbrain crest cells to the mesenchyme in the frontonasal mass of mouse embryos. *Dev. Biol.* **164**, 409-419.
Paek, H., Gutin, G. and Hebert, J. M. (2009). FGF signaling is strictly required to maintain early telencephalic precursor cell survival. *Development* **136**, 2457-2465.
Paek, H., Hwang, J. Y., Zukin, R. S. and Hebert, J. M. (2011). beta-Catenin-dependent FGF signaling sustains cell survival in the anterior embryonic head by countering Smad4. *Dev. Cell* **20**, 689-699.
Reid, B. S., Yang, H., Melvin, V. S., Taketo, M. M. and Williams, T. (2011). Ectodermal Wnt/beta-catenin signaling shapes the mouse face. *Dev. Biol.* **349**, 261-269.
Riley, B. M., Mansilla, M. A., Ma, J., Daack-Hirsch, S., Maher, B. S., Raffensperger, L. M., Russo, E. T., Vieira, A. R., Dode, C., Mohammadi, M. et al. (2007). Impaired FGF signaling contributes to cleft lip and palate. *Proc. Natl. Acad. Sci. USA* **104**, 4512-4517.
Sarkar, S., Petiot, A., Copp, A., Ferretti, P. and Thorogood, P. (2001). FGF2 promotes skeletogenic differentiation of cranial neural crest cells. *Development* **128**, 2143-2152.
Serbedzija, G. N., Bronner-Fraser, M. and Fraser, S. E. (1992). Vital dye analysis of cranial neural crest cell migration in the mouse embryo. *Development* **116**, 297-307.
Song, L., Li, Y., Wang, K., Wang, Y. Z., Molotkov, A., Gao, L., Zhao, T., Yamagami, T., Wang, Y., Gan, Q. et al. (2009). Lrp6-mediated canonical Wnt signaling is required for lip formation and fusion. *Development* **136**, 3161-3171.
Summerhurst, K., Stark, M., Sharpe, J., Davidson, D. and Murphy, P. (2008). 3D representation of Wnt and Frizzled gene expression patterns in the mouse embryo at embryonic day 11.5 (Ts19). *Gene Expr. Patterns* **8**, 331-348.
Szabo-Rogers, H. L., Smithers, L. E., Yakob, W. and Liu, K. J. (2010). New directions in craniofacial morphogenesis. *Dev. Biol.* **341**, 84-94.
Thomas, P. S., Kim, J., Nunez, S., Glogauer, M. and Kaartinen, V. (2010). Neural crest cell-specific deletion of Rac1 results in defective cell-matrix interactions and severe craniofacial and cardiovascular malformations. *Dev. Biol.* **340**, 613-625.
Trumpp, A., Depew, M. J., Rubenstein, J. L., Bishop, J. M. and Martin, G. R. (1999). Cre-mediated gene inactivation demonstrates that FGF8 is required for cell survival and patterning of the first branchial arch. *Genes Dev.* **13**, 3136-3148.
Wang, Y., Song, L. and Zhou, C. J. (2011). The canonical Wnt/beta-catenin signaling pathway regulates Fgf signaling for early facial development. *Dev. Biol.* **349**, 250-260.
Yamada, W., Nagao, K., Horikoshi, K., Fujikura, A., Ikeda, E., Inagaki, Y., Kakitani, M., Tomizuka, K., Miyazaki, H., Suda, T. et al. (2009). Craniofacial malformation in R-spondin2 knockout mice. *Biochem. Biophys. Res. Commun.* **381**, 453-458.
Yu, H., Smallwood, P. M., Wang, Y., Vidaltamayo, R., Reed, R. and Nathans, J. (2010). Frizzled 1 and frizzled 2 genes function in palate, ventricular septum and neural tube closure: general implications for tissue fusion processes. *Development* **137**, 3707-3717.